

Heat Focusing in Head and Neck Hyperthermia Considering Vessels Blood Flow

Original

Heat Focusing in Head and Neck Hyperthermia Considering Vessels Blood Flow / Firuzalizadeh, Maryam; Gaffoglio, Rossella; Giordanengo, Giorgio; Righero, Marco; Zucchi, Marcello; Musacchio Adorasio, Giuseppe; Bellone, Aurora; Vallan, Alberto; Perrone, Guido; Vecchi, Giuseppe. - ELETTRONICO. - (2025), pp. 1-4. (Intervento presentato al convegno 19th European Conference on Antennas and Propagation tenutosi a Stockholm (Swe) nel March 30 - April 4, 2025).

Availability:

This version is available at: 11583/2998905 since: 2025-04-10T10:04:41Z

Publisher:

IEEE

Published

DOI:

Terms of use:

This article is made available under terms and conditions as specified in the corresponding bibliographic description in the repository

Publisher copyright

IEEE postprint/Author's Accepted Manuscript

©2025 IEEE. Personal use of this material is permitted. Permission from IEEE must be obtained for all other uses, in any current or future media, including reprinting/republishing this material for advertising or promotional purposes, creating new collecting works, for resale or lists, or reuse of any copyrighted component of this work in other works.

(Article begins on next page)

Heat Focusing in Head and Neck Hyperthermia Considering Vessels Blood Flow

Maryam Firuzalizadeh¹, Rossella Gaffoglio², Giorgio Giordanengo², Marco Righero², Marcello Zucchi¹, Giuseppe Musacchio Adoriso², Aurora Bellone¹, Alberto Vallan¹, Guido Perrone¹, and Giuseppe Vecchi¹

¹Department of Electronics and Telecommunications, Politecnico di Torino, Torino, Italy,

{maryam.firuzalizadeh, marcello.zucchi, aurora.bellone, alberto.vallan, guido.perrone, giuseppe.vecchi}@polito.it

²Advanced Computing, Photonics & Electromagnetics (CPE), Fondazione LINKS, Torino, Italy,

{rossella.gaffoglio, giorgio.giordanengo, marco.righero, giuseppe.musacchio}@linksfoundation.com

Abstract—This paper investigates how blood flow in major vessels affects temperature distribution during hyperthermia treatments in the head and neck (H&N) region. To do this, we used an in-silico model and a physical phantom of the neck region where a silicon tube with flowing water was introduced to simulate the presence of the two jugular veins and two carotid arteries. The results show that temperature variations of more than 5°C can affect temperature simulations when the effect of blood flow is not considered. The achieved results were confirmed by temperature measurements performed using the physical phantom and a full-operating mock-up reproducing an hyperthermia treatment in the neck region.

Index Terms—Hyperthermia treatment (HT), specific absorption rate (SAR), hyperthermia treatment planning (HTP), tissue mimicking materials (TMMs).

I. INTRODUCTION

Tissue mimicking materials (TMMs) are essential in medical research, providing a platform to test new devices and techniques without risks to humans or animals [1]. These materials, typically incorporated into phantoms, replicate human tissue properties and are invaluable in clinical simulations for imaging, therapy, and device performance validation. Microwave hyperthermia (HT) is among the medical applications requiring phantoms for design and testing. This therapy is a complementary cancer treatment aimed at selectively increasing the temperature of tumor cells to 40-44°C using antenna array systems [2].

However, one of the primary challenges in optimizing HT is accurately modeling heat transfer in biological tissues, where the effect of blood plays a critical role in temperature regulation. Despite significant advances in TMMs, the absence of physical phantoms for hyperthermia reproducing the effects of the blood system has limited experimental validation [1].

This gap limits the ability to experimentally validate and optimize microwave hyperthermia treatments, leaving researchers to rely heavily on computational models to simulate blood flow and its thermal effects.

The present study introduces a head and neck (H&N) phantom that incorporates major vessels, i.e., the jugular veins and carotid arteries, to simulate blood flow at different fluid velocities. This allows for the assessment of vascular dynamics' impact on temperature focusing during microwave hyperthermia. While blood vessels have almost no

effects on SAR focusing, their presence causes changes in the temperature maps due to the cooling effect of the flowing blood. Vessels introduce in fact thermal boundary conditions which can determine deviations of the temperature distribution compared to the corresponding specific absorption rate (SAR) map [3].

II. METHODOLOGY

The designed experimental setup represents a common hyperthermia (HT) applicator for deep-seated and sub-superficial tumors in the H&N region [4], [5], operating at the central frequency $f = 434$ MHz. The setup, as shown in Fig. 1, consists of a circular array of $N = 8$ patch antennas with water substrate, surrounding a central Poly(methyl methacrylate) (PMMA) cylinder designed to represent the neck phantom. Inside this phantom, a red sphere was placed to represent the tumor target, and silicone tubes were used to simulate the major blood vessels, specifically the two jugular veins and two carotid arteries. Additionally, the neck phantom contains one solid and one hollow PMMA cylinder, simulating the spine and trachea, respectively. The neck phantom was then filled with an in-house agar-based mixture, formulated to mimic the dielectric and thermal properties of human muscle tissue, as described in [6].

The in-silico model of this setup was implemented in COMSOL Multiphysics[®] [7], as shown in Fig. 2a. The cross-sectional view of the phantom, illustrated in Fig. 2b, shows the placement of four tubes that simulate the blood vessels. The center coordinates and diameters of these vessels, along with the tumor target, are provided in Table I. To simulate blood flow, water was circulated through the tubes at controlled

TABLE I
Center coordinates and diameters of key elements within the neck phantom

Element	x (mm)	y (mm)	d (mm)
Right Jugular vein	-45	0	4
Left Jugular vein	+45	0	4
Right carotid artery	-40	-15	4
Left carotid artery	+40	-15	4
Tumor target	-20	-18	25

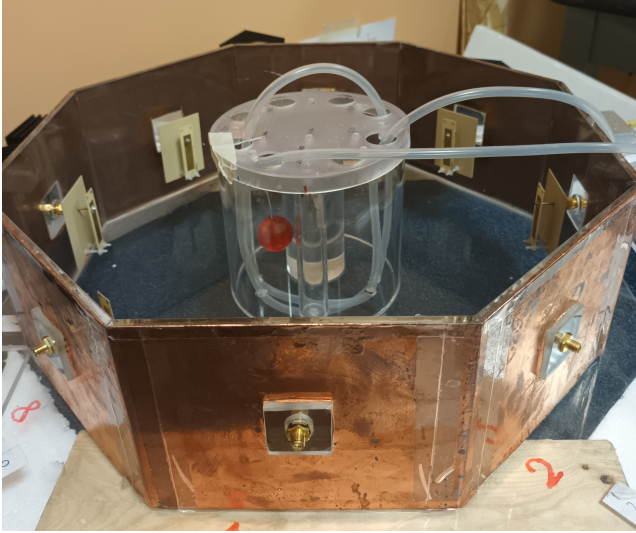


Fig. 1. Experimental setup of the mock-up reproducing the HT applicator. The central section contains the agar-based phantom (not visualized in the picture), including silicone tubes simulating blood vessels and a red sphere representing the tumor target.

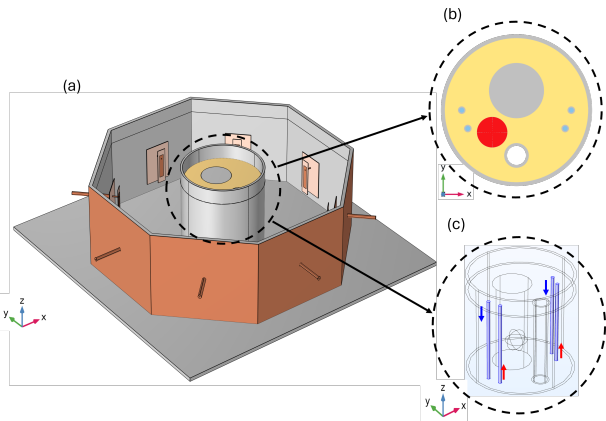


Fig. 2. (a) In-silico model of the experimental setup realized in COMSOL Multiphysics. (b) Cross-sectional view in the xy plane of the neck phantom, showing the tubes simulating blood vessels: 1- Right jugular vein, 2- Left jugular vein, 3- Right carotid artery, 4- Left carotid artery. (c) 3D visualization of the neck phantom, illustrating the vessels and fluid flow direction.

velocities $v = 30$ cm/s [8], [9], as visualized in Fig. 2c, enabling the analysis of vascular effects on heat distribution.

To reproduce a hyperthermia treatment session using the realized mock-up following the hyperthermia treatment planning (HTP), we employed a SAR-based optimization approach, as described in [10], to determine the optimal set of antenna coefficients that maximize power deposition in the target region within the neck phantom. In this SAR-based optimization, the electric fields generated by each antenna in the array, when acting individually, were calculated using COMSOL Multiphysics. These individual fields were then combined through a superposition of unknown feeding coefficients; in the presented paper, only the phases φ_n , $n = 1, \dots, N$, were

considered for simplicity.

Then, a particle swarm optimization (PSO) was performed in MATLAB [11] to find the feeding coefficients that maximize power deposition in the target region and minimize the risk of hotspots in surrounding healthy tissues. An additional condition was also imposed to prevent the excessive reflected power and avoid damaging the setup electronic equipment.

The resulting optimized phase coefficients for the antenna array, along with the simulated active reflection coefficients, are reported in Table II.

III. RESULTS AND DISCUSSION

The simulated SAR distribution corresponding to the optimized set of phases (see Table II) is shown in Fig. 3, for an input power $P_0 = 75$ W and a water velocity $v = 30$ cm/s in the silicone tubes. As can be observed, effective SAR focusing is achieved on the tumor target.

While the presence of the blood vessels has negligible influence on the SAR distribution, the temperature map resulted by the deposited SAR is strongly influenced by the cooling effect of flowing water in the vessels, which simulates the heat dissipation from blood flow in vivo.

Fig. 4 reports the simulated temperature profiles in the phantom, for different values of the water velocity. The top row shows the temperature profiles at the fixed coordinate $z = 0$ mm (which corresponds to the tumor center) as function of time, at different positions on the xy plane, while the bottom row reports the temperature distribution at a fixed time ($t = 120$) for different points along the z -axis. It is observed that using a non-zero velocity ($v \neq 0$ cm/s) produces different temperature distributions compared to static conditions. However, increasing the velocity beyond 10 cm/s does not significantly alter the results, indicating that the presence of flow has a more critical impact than the specific velocity magnitude.

To experimentally demonstrate the impact of blood vessels in the temperature distribution, a heating session was conducted in which arrays of Fiber Optic Sensors (FOS), consisting of Fiber Bragg Grating (FBG) sensors, were used to measure the temperature distribution along the vertical z -axis at various positions within the phantom. Results concerning the experimental validation will be presented during the Conference.

TABLE II
Optimized antenna phases and simulated active reflection coefficients

n	φ_n ($^\circ$)	$\Gamma_{n,sim}^a$ (dB)
1	0	-22.15
2	82.38	-10.41
3	164.45	-10.40
4	-143.79	-10.63
5	-116.35	-10.53
6	6.03	-19.18
7	-20.17	-20.05
8	-31.61	-18.22

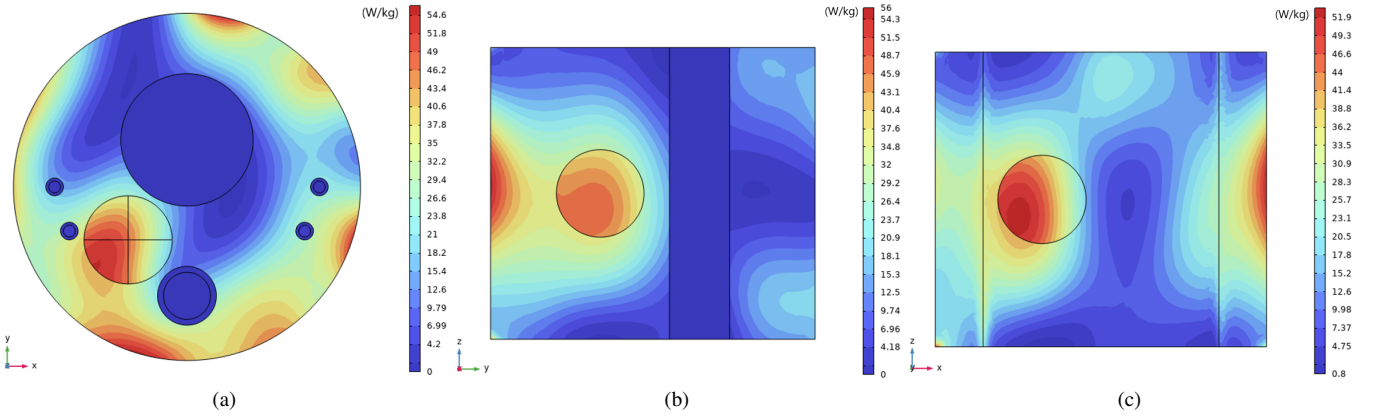


Fig. 3. Optimized SAR distribution simulated in COMSOL Multiphysics in the presence of silicon tubes representing the vessels. The SAR maps are displayed on the three canonical planes cutting the tumor sphere at its centroid.

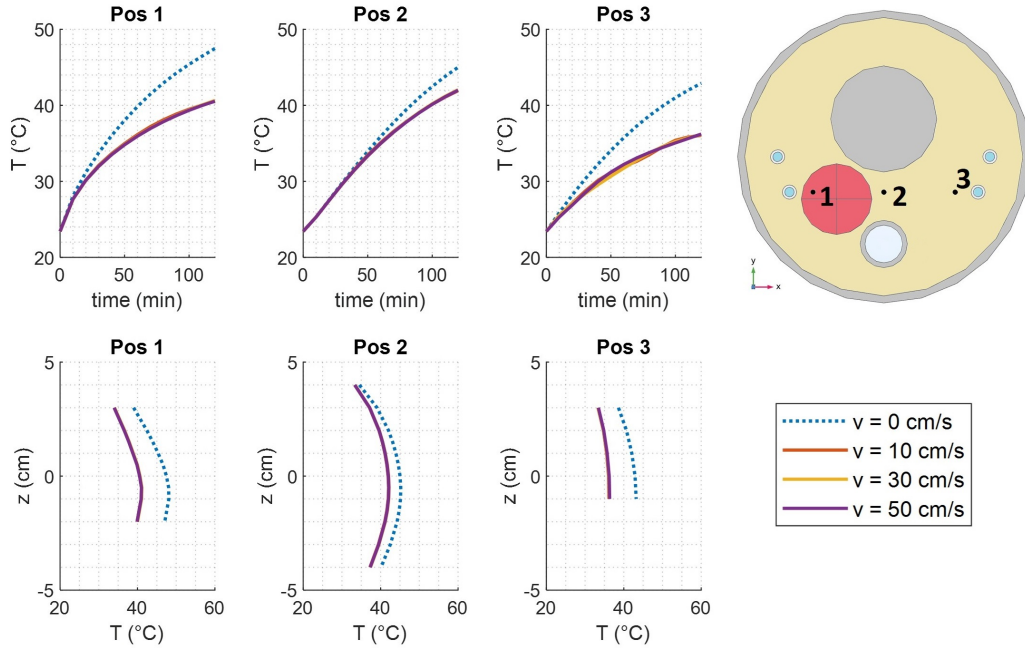


Fig. 4. Simulated temperature for different water velocities in the tubes. Top panels show the temperature at the height of the tumor center ($z = 0$ mm) as a function of time t ; bottom panels show temperature as a function of z at the end of the heating session ($t = 120$ min).

IV. CONCLUSION

This study underscores the importance of incorporating a vascular model within the phantom for microwave hyperthermia treatment for deep-seated tumors in the head and neck region. The results demonstrate how the presence of blood flow affects temperature maps starting from a certain SAR distribution. This shows how this effect should be included in simulations and physical phantoms to achieve more realistic temperature predictions.

While these results are promising, some limitations of the current model have been identified, such as simplifications in the dynamics of blood vessels. Future studies should aim to investigate variable vessel geometries, to reproduce a more detailed discrete vasculature, and to design a more realistic anatomical model.

ACKNOWLEDGMENT

This work was partially supported by the project “Real-Time Temperature Maps Reconstruction in Microwave Cancer Hyperthermia”, Proof of Concept (PoC) Instrument Linea 3 – PoC EIC.

REFERENCES

- [1] C. K. McGarry, L. J. Grattan, A. M. Ivory, F. Leek, G. P. Liney, Y. Liu, P. Miloro, R. Rai, A. Robinson, A. J. Shih, B. Zeqiri, and C. H. Clark, “Tissue mimicking materials for imaging and therapy phantoms: a review,” *Phys. Med. Biol.*, 2020.
- [2] N. R. Datta, S. Rogers, D. Klingbiel, S. Gómez, E. Puric, and S. Bodis, “Hyperthermia and radiotherapy with or without chemotherapy in locally advanced cervical cancer: a systematic review with conventional and network meta analyses,” *Int. J. of Hyperthermia*, vol. 32, no. 7, pp. 809–21, 2016.

- [3] R. Gaffoglio, M. Righero, G. Giordanengo, M. Zucchi, and G. Vecchi, "Fast optimization of temperature focusing in hyperthermia treatment of sub-superficial tumors," *IEEE J. Electromagn. RF Microw. Med. Biol.*, vol. 5, no. 3, pp. 286–93, 2021.
- [4] M. M. Paulides *et al.*, "The HYPERcollar: A novel applicator for hyperthermia in the head and neck," *Int. J. Hyperthermia*, vol. 23, no. 7, pp. 567–76, 2007.
- [5] M. M. Paulides, J. F. Bakker, A. P. M. Zwamborn, and G. C. Van Rhoon, "A head and neck hyperthermia applicator: theoretical antenna array design," *Int. J. Hyperthermia*, vol. 23, no. 1, pp. 59–67, 2007.
- [6] R. Gaffoglio, M. Firuzalizadeh, G. Giordanengo, M. Righero, M. Zucchi, G. Adoriso, and G. Vecchi, "Highly reproducible tissue-mimicking phantoms for hyperthermia applications," in *Proceedings of IEEE Antennas and Propagation Society International Symposium and URSI National Radio Science Meeting*, vol. 1, no. 07, 2024, pp. 1–2.
- [7] COMSOL Multiphysics, *version 6.2*. www.comsol.it, 2024.
- [8] L. A. Ferrara, M. Mancini, R. Iannuzzi, T. Marotta, I. Gaeta, F. Pasanisi, A. Postiglione, and L. Guida, "Carotid diameter and blood flow velocities in cerebral circulation in hypertensive patients," *Stroke*, vol. 26, no. 3, pp. 418–421, 1995.
- [9] G. Ciuti, D. Righi, L. Forzoni, A. Fabbri, and A. M. Pignone, "Differences between internal jugular vein and vertebral vein flow examined in real time with the use of multigate ultrasound color Doppler," *AJNR Am J Neuroradiol*, vol. 34, no. 10, pp. 2000–2004, 2013.
- [10] Z. Rijnen *et al.*, "Clinical integration of software tool VEDO for adaptive and quantitative application of phased array hyperthermia in the head and neck," *Int. J. Hyperthermia*, vol. 29, no. 3, pp. 181–93, 2013.
- [11] MATLAB. Natick, Massachusetts: The MathWorks Inc., 2023.